

D_s^+ Exclusive Hadronic Decays Involving ω

J. Y. Ge,¹ D. H. Miller,¹ I. P. J. Shipsey,¹ B. Xin,¹ G. S. Adams,² D. Hu,² B. Moziak,²
 J. Napolitano,² K. M. Ecklund,³ Q. He,⁴ J. Insler,⁴ H. Muramatsu,⁴ C. S. Park,⁴
 E. H. Thorndike,⁴ F. Yang,⁴ M. Artuso,⁵ S. Blusk,⁵ S. Khalil,⁵ R. Mountain,⁵
 K. Randrianarivony,⁵ T. Skwarnicki,⁵ S. Stone,⁵ J. C. Wang,⁵ L. M. Zhang,⁵ G. Bonvicini,⁶
 D. Cinabro,⁶ A. Lincoln,⁶ M. J. Smith,⁶ P. Zhou,⁶ J. Zhu,⁶ P. Naik,⁷ J. Rademacker,⁷
 D. M. Asner,⁸ K. W. Edwards,⁸ J. Reed,⁸ A. N. Robichaud,⁸ G. Tatishvili,⁸ E. J. White,⁸
 R. A. Briere,⁹ H. Vogel,⁹ P. U. E. Onyisi,¹⁰ J. L. Rosner,¹⁰ J. P. Alexander,¹¹
 D. G. Cassel,¹¹ R. Ehrlich,¹¹ L. Fields,¹¹ L. Gibbons,¹¹ S. W. Gray,¹¹ D. L. Hartill,¹¹
 B. K. Heltsley,¹¹ J. M. Hunt,¹¹ J. Kandaswamy,¹¹ D. L. Kreinick,¹¹ V. E. Kuznetsov,¹¹
 J. Ledoux,¹¹ H. Mahlke-Krüger,¹¹ J. R. Patterson,¹¹ D. Peterson,¹¹ D. Riley,¹¹ A. Ryd,¹¹
 A. J. Sadoff,¹¹ X. Shi,¹¹ S. Stroiney,¹¹ W. M. Sun,¹¹ T. Wilksen,¹¹ J. Yelton,¹² P. Rubin,¹³
 N. Lowrey,¹⁴ S. Mehrabyan,¹⁴ M. Selen,¹⁴ J. Wiss,¹⁴ M. Kornicer,¹⁵ R. E. Mitchell,¹⁵
 M. R. Shepherd,¹⁵ C. M. Tarbert,¹⁵ D. Besson,¹⁶ T. K. Pedlar,¹⁷ J. Xavier,¹⁷
 D. Cronin-Hennessy,¹⁸ K. Y. Gao,¹⁸ J. Hietala,¹⁸ T. Klein,¹⁸ R. Poling,¹⁸ P. Zweber,¹⁸
 S. Dobbs,¹⁹ Z. Metreveli,¹⁹ K. K. Seth,¹⁹ B. J. Y. Tan,¹⁹ A. Tomaradze,¹⁹ S. Brisbane,²⁰
 J. Libby,²⁰ L. Martin,²⁰ A. Powell,²⁰ C. Thomas,²⁰ G. Wilkinson,²⁰ and H. Mendez²¹

(CLEO Collaboration)

¹*Purdue University, West Lafayette, Indiana 47907, USA*²*Rensselaer Polytechnic Institute, Troy, New York 12180, USA*³*Rice University, Houston, Texas 77005, USA*⁴*University of Rochester, Rochester, New York 14627, USA*⁵*Syracuse University, Syracuse, New York 13244, USA*⁶*Wayne State University, Detroit, Michigan 48202, USA*⁷*University of Bristol, Bristol BS8 1TL, UK*⁸*Carleton University, Ottawa, Ontario, Canada K1S 5B6*⁹*Carnegie Mellon University, Pittsburgh, Pennsylvania 15213, USA*¹⁰*University of Chicago, Chicago, Illinois 60637, USA*¹¹*Cornell University, Ithaca, New York 14853, USA*¹²*University of Florida, Gainesville, Florida 32611, USA*¹³*George Mason University, Fairfax, Virginia 22030, USA*¹⁴*University of Illinois, Urbana-Champaign, Illinois 61801, USA*¹⁵*Indiana University, Bloomington, Indiana 47405, USA*¹⁶*University of Kansas, Lawrence, Kansas 66045, USA*¹⁷*Luther College, Decorah, Iowa 52101, USA*¹⁸*University of Minnesota, Minneapolis, Minnesota 55455, USA*¹⁹*Northwestern University, Evanston, Illinois 60208, USA*²⁰*University of Oxford, Oxford OX1 3RH, UK*²¹*University of Puerto Rico, Mayaguez, Puerto Rico 00681*

(Dated: June 11, 2009)

Abstract

Using data collected near the $D_s^{*\pm}D_s^\mp$ peak production energy $E_{\text{cm}} = 4170$ MeV by the CLEO-c detector, we search for D_s^+ exclusive hadronic decays involving ω . We find $\mathcal{B}(D_s^+ \rightarrow \pi^+\omega) = (0.21 \pm 0.09 \pm 0.01)\%$, $\mathcal{B}(D_s^+ \rightarrow \pi^+\pi^0\omega) = (2.78 \pm 0.65 \pm 0.25)\%$, $\mathcal{B}(D_s^+ \rightarrow \pi^+\pi^+\pi^-\omega) = (1.58 \pm 0.45 \pm 0.09)\%$, $\mathcal{B}(D_s^+ \rightarrow \pi^+\eta\omega) = (0.85 \pm 0.54 \pm 0.06)\%$, $\mathcal{B}(D_s^+ \rightarrow K^+\omega) < 0.24\%$, $\mathcal{B}(D_s^+ \rightarrow K^+\pi^0\omega) < 0.82\%$, $\mathcal{B}(D_s^+ \rightarrow K^+\pi^+\pi^-\omega) < 0.54\%$, and $\mathcal{B}(D_s^+ \rightarrow K^+\eta\omega) < 0.79\%$. The upper limits are at 90% confidence level.

The inclusive ω yield, $D_s^+ \rightarrow \omega X$, is substantial $(6.1 \pm 1.4)\%$ [1]. This is very surprising, as the only D_s^+ exclusive decay mode involving ω that has been observed is $D_s^+ \rightarrow \pi^+\omega$, with a branching fraction of $\mathcal{B}(D_s^+ \rightarrow \pi^+\omega) = (0.25 \pm 0.09)\%$ [2]. There is lots of room for more D_s^+ exclusive hadronic decays involving ω . The study of ω production in D_s^+ decays is of interest in shedding light on mechanisms of weak decay and their interplay with long-distance (nonperturbative) physics [3]. Here we present a search for several D_s^+ exclusive hadronic decays involving ω . In particular, we consider final states with one, two, and three pions: $D_s^+ \rightarrow \pi^+\omega$, $D_s^+ \rightarrow \pi^+\pi^0\omega$, and $D_s^+ \rightarrow \pi^+\pi^+\pi^-\omega$. We also search for $D_s^+ \rightarrow \pi^+\eta\omega$, as this has been suggested [3] as possibly being a large decay mode. Finally, we search for modes in which one of the π^+ from the above-mentioned decays is replaced by a K^+ : $D_s^+ \rightarrow K^+\omega$, $D_s^+ \rightarrow K^+\pi^0\omega$, $D_s^+ \rightarrow K^+\pi^+\pi^-\omega$, and $D_s^+ \rightarrow K^+\eta\omega$. These last four modes would be Cabibbo-suppressed, and hence are not expected to be large.

In this study we use 586 pb^{-1} of data produced in e^+e^- collisions at the Cornell Electron Storage Ring (CESR) and collected by the CLEO-c detector near the center-of-mass (CM) energy $\sqrt{s} = 4170 \text{ MeV}$. At this energy the cross-section for the channel of interest, $D_s^{*+}D_s^-$ or $D_s^+D_s^{*-}$, is approximately 1 nb [4]. We select events in which the D_s^* decays to $D_s\gamma$ (94% branching fraction [2]). Other charm production totals $\sim 7 \text{ nb}$ [4], and the underlying light-quark “continuum” is about 12 nb .

The CLEO-c detector is a general-purpose solenoidal detector, which is described in detail elsewhere [5–8]. The charged particle tracking system covers a solid angle of 93% of 4π and consists of a small-radius, six-layer, low-mass, stereo wire drift chamber, concentric with, and surrounded by, a 47-layer cylindrical central drift chamber. The chambers operate in a 1.0 T magnetic field. The root-mean-square (rms) momentum resolution achieved with the tracking system is approximately 0.6% at $p = 1 \text{ GeV}/c$ for tracks that traverse all layers of the drift chamber. Photons are detected in an electromagnetic calorimeter consisting of about 7800 CsI(Tl) crystals [6]. The calorimeter attains an rms photon energy resolution of 2.2% at $E_\gamma = 1 \text{ GeV}$ and 5% at 100 MeV. The solid angle coverage for neutral particles in the CLEO-c detector is 93% of 4π . We utilize two particle identification (PID) devices to separate charged kaons from pions: the central drift chamber, which provides measurements of ionization energy loss (dE/dx), and, surrounding this drift chamber, a cylindrical ring-imaging Cherenkov (RICH) detector, whose active solid angle is 80% of 4π . The combined PID system has a pion or kaon efficiency $> 85\%$ and a probability of pions faking kaons (or vice versa) $< 5\%$ [9]. The detector response is modeled with a detailed GEANT-based [10] Monte Carlo (MC) simulation, with initial particle trajectories generated by EvtGen [11] and final state radiation produced by PHOTOS [12]. The modeling of initial-state radiation is based on cross sections for $D_s^{*\pm}D_s^\mp$ production at lower energies obtained from the CLEO-c energy scan [4] near the CM energy where we collected the sample.

Here we employ a double-tagging technique, the same as the technique that is used in the D_s^+ inclusive decay analysis [1]. Single-tag (ST) events are selected by fully reconstructing a D_s^- , which we call a tag, in one of the following three two-body hadronic decay modes: $D_s^- \rightarrow K_S^0 K^-$, $D_s^- \rightarrow \phi\pi^-$ and $D_s^- \rightarrow K^{*0}K^-$. (Mention of a specific mode implies the use of the charge conjugate mode as well throughout this Letter.) Details on the tagging selection procedure are given in Refs. [1, 13, 14]. The tagged D_s^- candidate can be either the primary D_s^- or the secondary D_s^- from the decay $D_s^{*-} \rightarrow \gamma D_s^-$. We require the resonance decays to satisfy the following mass windows around the nominal masses [2]: $K_S^0 \rightarrow \pi^+\pi^-$ ($\pm 12 \text{ MeV}$), $\phi \rightarrow K^+K^-$ ($\pm 10 \text{ MeV}$) and $K^{*0} \rightarrow K^+\pi^-$ ($\pm 75 \text{ MeV}$). The momenta of all charged particles utilized in tags are required to be $100 \text{ MeV}/c$ or greater to suppress the

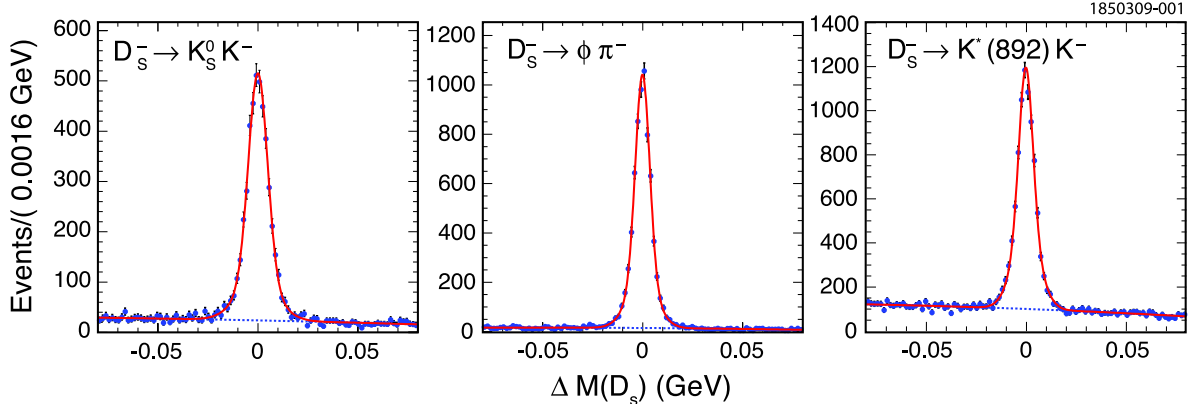


FIG. 1: The mass difference $\Delta M(D_s) \equiv M(D_s) - m_{D_s}$ distributions in each tag mode. We fit the $\Delta M(D_s)$ distribution (points) to the sum (solid curve) of signal (double-Gaussian) plus background (second degree polynomial, dashed curve) functions.

slow pion background from $D^* \bar{D}^*$ and $D^* D$ decays (through $D^* \rightarrow \pi D$).

The reconstructed invariant mass of the D_s candidate, $M(D_s)$, and the mass recoiling against the D_s candidate, $M_{\text{recoil}}(D_s) \equiv \sqrt{(E_0 - E_{D_s})^2 - (\mathbf{p}_0 - \mathbf{p}_{D_s})^2}$, are used as our primary kinematic variables to select a D_s candidate. Here (E_0, \mathbf{p}_0) is the net four-momentum of the e^+e^- beams, taking the finite beam crossing angle into account, \mathbf{p}_{D_s} is the momentum of the D_s candidate, $E_{D_s} = \sqrt{m_{D_s}^2 + \mathbf{p}_{D_s}^2}$, and m_{D_s} is the known D_s mass [2]. We require the recoil mass to be within 55 MeV of the D_s^* mass [2]. This loose window allows both primary and secondary D_s tags to be selected. We also require a photon consistent with coming from $D_s^* \rightarrow \gamma D_s$ decay, by looking at the mass recoiling against the D_s candidate plus γ system, $M_{\text{recoil}}(D_s \gamma) \equiv \sqrt{(E_0 - E_{D_s} - E_\gamma)^2 - (\mathbf{p}_0 - \mathbf{p}_{D_s} - \mathbf{p}_\gamma)^2}$. For correct combinations, this recoil mass peaks at m_{D_s} , regardless of whether the candidate is due to a primary or a secondary D_s . We require $|M_{\text{recoil}}(D_s \gamma) - m_{D_s}| < 30$ MeV.

The distributions of $\Delta M(D_s) \equiv M(D_s) - m_{D_s}$, the invariant mass difference of D_s tag candidates, after applying the two recoil mass requirements for each tag mode are shown Fig. 1. We use the tag invariant mass sidebands to estimate the backgrounds in our signal yields from the wrong tag combinations (incorrect combinations that, by chance, lie within the $\Delta M(D_s)$ signal region). The signal region is $|\Delta M(D_s)| < 20$ MeV, while the sideband region is $35 \text{ MeV} < |\Delta M(D_s)| < 55$ MeV. To find the sideband scaling factor, the $\Delta M(D_s)$ distributions are fit to the sum of double-Gaussian signal plus second-degree polynomial background functions. We have 18586 ± 163 ST events that we use for further analysis.

In each event where a tag is identified, we search for our signal modes recoiling against the tag. Charged tracks utilized in signal candidates are required to satisfy criteria based on the track fit quality, have momenta above 50 MeV/c, and angles θ with respect to the beam line, satisfying $|\cos \theta| < 0.93$. They must also be consistent with coming from the interaction point in three dimensions. Pion and kaon candidates are required to have dE/dx measurements within three standard deviations (3σ) of the expected value. For tracks with momenta greater than 700 MeV/c, RICH information, if available, is combined with dE/dx .

We identify π^0 candidates via $\pi^0 \rightarrow \gamma\gamma$, detecting the photons in the CsI calorimeter. To avoid having both photons in a region of poorer energy resolution, we require that at least one of the photons be in the ‘‘good barrel’’ region, $|\cos \theta_\gamma| < 0.8$. We require that

the calorimeter clusters have a measured energy above 30 MeV, have a lateral distribution consistent with that from photons, and not be matched to any charged track. The invariant mass of the photon pair is required to be within 3σ ($\sigma \sim 6$ MeV) of the known π^0 mass. The η candidates are formed using a similar procedure as for π^0 except that $\sigma \sim 12$ MeV. The π^0 and η mass constraints are imposed when π^0 or η candidates are used in further reconstruction. We reconstruct ω candidates in the $\omega \rightarrow \pi^+\pi^-\pi^0$ decay mode.

Mode-dependent requirements on numbers of charged kaons and pions are applied on the signal side. For example, we require there must be exactly one charged kaon and two charged pions for the $D_s^+ \rightarrow K^+\omega, \omega \rightarrow \pi^+\pi^-\pi^0$ mode. No extra tracks are allowed on the signal side. The best π^0 (or η) candidate is selected based on the pull mass (number of standard deviations of measured mass from true mass). For $D_s^+ \rightarrow \pi^+\eta\omega$, a veto on $\eta' \rightarrow \pi^+\pi^-\eta$ has been applied to remove the dominant background contribution from the $D_s^+ \rightarrow \pi^+\pi^0\eta'$ decay.

The double-tag (DT) yields are extracted from the $\pi^+\pi^-\pi^0$ invariant mass distribution after requiring that both the tagging D_s and signal D_s invariant masses be in the D_s nominal mass region (20 MeV mass window on the tag side and 30 MeV mass window on the signal side due to π^0 or η on the signal side). The ω mass signal region is $|M_{\pi^+\pi^-\pi^0} - m_\omega| < 20$ MeV, while the sideband region is $40 \text{ MeV} < |M_{\pi^+\pi^-\pi^0} - m_\omega| < 80$ MeV, where $M_{\pi^+\pi^-\pi^0}$ is the $\pi^+\pi^-\pi^0$ invariant mass and m_ω is the nominal mass of ω [2].

The invariant mass distributions of ω candidates for the first four modes are shown in Fig. 2 and the yields are given in Table I. For $D_s^+ \rightarrow \pi^+\omega$, $D_s^+ \rightarrow \pi^+\pi^0\omega$, and $D_s^+ \rightarrow \pi^+\pi^+\pi^-\omega$, clear signals are found in the data. Note also the peaks from $\eta \rightarrow \pi^+\pi^-\pi^0$ and $\phi \rightarrow \pi^+\pi^-\pi^0$, corresponding to known D_s decays to η plus pions and ϕ plus pions.

For $D_s^+ \rightarrow \pi^+\eta\omega$, we observe 7 events in the signal region, and 5 events in a sideband region twice as wide. From Binomial statistics, the probability of observing 7 or more events in the signal region and 5 or fewer events in the sideband region, out of a total of 12 events, if there is no true signal, is 6.6%. Thus we have ‘‘evidence’’ for $D_s^+ \rightarrow \pi^+\eta\omega$, but cannot claim ‘‘observation’’. We quote both a value for the branching fraction and an upper limit on it.

We find no significant evidence for any of the modes with kaons, and therefore set upper limits on their branching fractions. The numbers of events from ω mass signal and sideband regions for these four modes are given in Table I. Upper limits are calculated using Poisson statistics, and allowing for uncertainty in number of background events.

We determine the efficiency for detecting our tags (ϵ_{ST}) using Monte Carlo samples in which one D_s decays into the tag mode, and the other decays generically. The single-tag efficiency weighted over the three tags is $(26.63 \pm 0.14)\%$. We determine the efficiency for detecting both tag and signal (ϵ_{DT}) using Monte Carlo samples in which one D_s decays into a tag mode, and the other D_s decays into a signal mode. For the three-body decay modes, we assume three-body phase space. For $D_s^+ \rightarrow \pi^+\pi^0\omega$, we also consider $D_s^+ \rightarrow \rho^+\omega, \rho^+ \rightarrow \pi^+\pi^0$. For $D_s^+ \rightarrow K^+\pi^0\omega$, we also consider $D_s^+ \rightarrow K^{*+}\omega, K^{*+} \rightarrow K^+\pi^0$. For $D_s^+ \rightarrow \pi^+\pi^+\pi^-\omega$, we assume $\pi^+\pi^+\pi^-\omega$ phase space and estimate a systematic error by using $D_s^+ \rightarrow \pi^+\rho^0\omega, \rho^0 \rightarrow \pi^+\pi^-$. Double-tag detection efficiencies are given in Table I.

The absolute branching fractions ($\mathcal{B}_{\text{mode}}$) are obtained from the ST yield (N_{ST}) and DT yield (N_{DT}) without needing to know the integrated luminosity or the produced number of $D_s^{*\pm}D_s^\mp$ pairs,

$$\mathcal{B}_{\text{mode}} = \frac{N_{\text{DT}}}{N_{\text{ST}}} \times \frac{\epsilon_{\text{ST}}}{\epsilon_{\text{DT}}}. \quad (1)$$

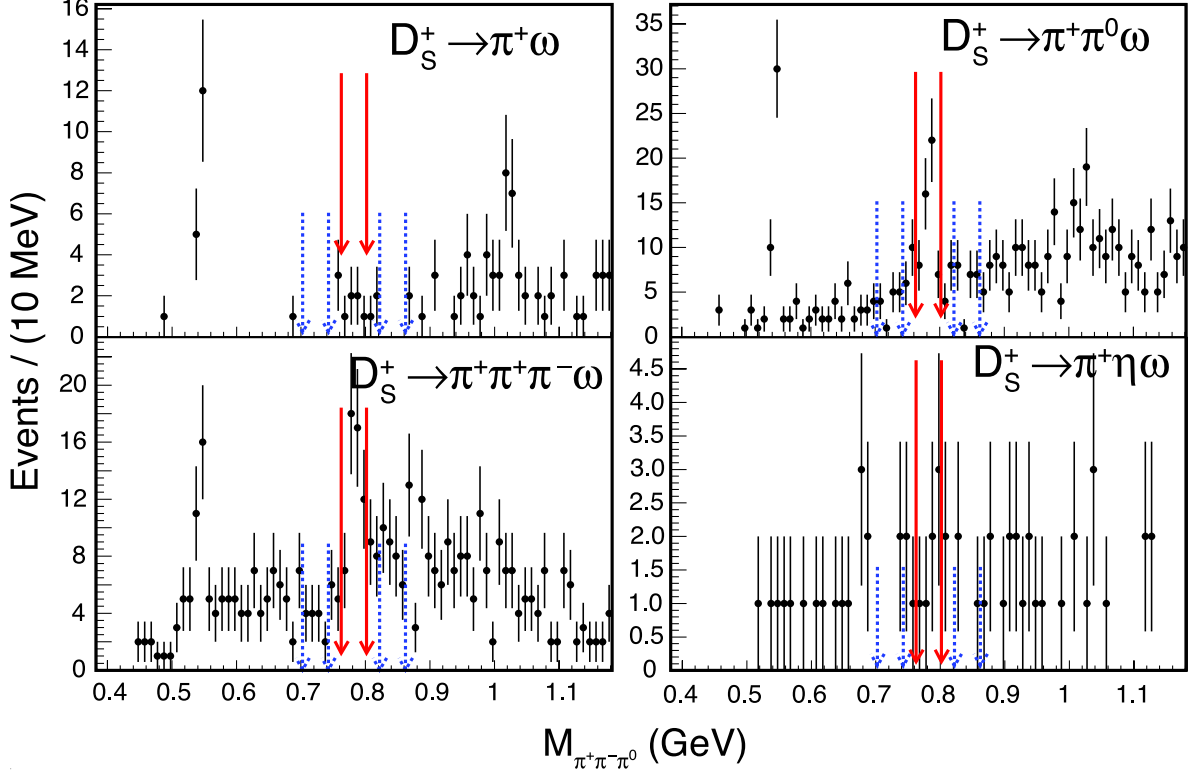


FIG. 2: Invariant mass distributions of ω candidates for the first four modes: $D_s^+ \rightarrow \pi^+\omega$, $D_s^+ \rightarrow \pi^+\pi^0\omega$, $D_s^+ \rightarrow \pi^+\pi^+\pi^-\omega$, and $D_s^+ \rightarrow \pi^+\eta\omega$. The solid lines (red online) indicate the ω mass signal region and the dashed lines (blue online) indicate the ω mass sideband regions. Peaks from $\eta \rightarrow \pi^+\pi^-\pi^0$ and $\phi \rightarrow \pi^+\pi^-\pi^0$ are also evident.

The $D_s^+ \rightarrow \pi^+\pi^0\omega$ decay might come from $D_s^+ \rightarrow \rho^+(\pi^+\pi^0)\omega$. We fit the corresponding $\pi^+\pi^0$ invariant mass distribution to the sum of phase space $\pi^+\pi^0\omega$ MC and $\rho^+\omega$ MC. The fit result suggests that 0.52 ± 0.30 of the $D_s^+ \rightarrow \pi^+\pi^0\omega$ decay come from the $D_s^+ \rightarrow \rho^+\omega$, $\rho^+ \rightarrow \pi^+\pi^0$ decay, as shown in Fig. 3.

We have considered several sources of systematic uncertainty. The uncertainty associated with the efficiency for finding a track is 0.3%; an additional 0.6% systematic uncertainty for each kaon track is added [9]. The relative systematic uncertainties for π^0 and η efficiencies are 4.0%. Uncertainties in the charged pion and kaon identification efficiencies are 0.3% per pion and 0.3% per kaon [9]. For the $D_s^+ \rightarrow \pi^+\pi^0\omega$ mode, the relative contribution of $D_s^+ \rightarrow \rho^+\omega$, $\rho^+ \rightarrow \pi^+\pi^0$ is determined to be 0.52 ± 0.30 from the fit. We use the central value of that ratio to calculate the efficiency and take the error as a systematic uncertainty. All Monte Carlo efficiencies have been corrected to include several known small differences between data and Monte Carlo simulation. Upper limits have been increased to allow for the systematic errors.

The branching fractions and upper limits are listed in Table II. In summary, we report first observations of $D_s^+ \rightarrow \pi^+\pi^0\omega$ and $D_s^+ \rightarrow \pi^+\pi^+\pi^-\omega$ decays. The branching fractions are substantial. We find evidence for the $D_s^+ \rightarrow \pi^+\eta\omega$ decay. Our measurement of $D_s^+ \rightarrow \pi^+\omega$ decay is in good agreement with the PDG value [2], and of comparable accuracy. The sum of branching fractions of these four observed modes is $(5.4 \pm 1.0)\%$, which accounts for

TABLE I: Observed yields. Here N_{Sg} is the observed event number from ω mass signal region, N_{Sd} is the scaled event number from ω mass sideband regions, and N_{Ss} is the sideband-subtracted signal yield. Double-tag detection efficiencies (ϵ_{DT}) are listed in the last column. The efficiencies include sub-mode branching fractions [2], and have been corrected to include several known small differences between data and Monte Carlo simulation. Errors shown are statistical errors only.

Mode	N_{Sg}	N_{Sd}	N_{Ss}	$\epsilon_{\text{DT}}(\%)$
$D_s^+ \rightarrow \pi^+\omega$	6.0	0.0	6.0 ± 2.4	4.07 ± 0.08
$D_s^+ \rightarrow \pi^+\pi^0\omega$	53.0	19.0	34.0 ± 7.9	1.75 ± 0.04
$D_s^+ \rightarrow \pi^+\pi^+\pi^-\omega$	54.0	24.8	29.2 ± 8.2	2.64 ± 0.07
$D_s^+ \rightarrow \pi^+\eta\omega$	7.0	2.5	4.5 ± 2.9	0.76 ± 0.04
$D_s^+ \rightarrow K^+\omega$	3.0	2.0	1.0 ± 2.0	3.66 ± 0.08
$D_s^+ \rightarrow K^+\pi^0\omega$	4.0	2.5	1.5 ± 2.3	1.32 ± 0.05
$D_s^+ \rightarrow K^+\pi^+\pi^-\omega$	3.0	1.5	1.5 ± 1.9	1.72 ± 0.05
$D_s^+ \rightarrow K^+\eta\omega$	0.0	0.0	0.0 ± 0.0	0.45 ± 0.03

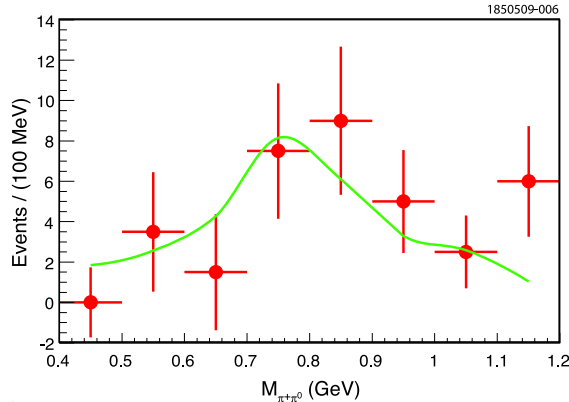


FIG. 3: $\pi^+\pi^0$ invariant mass distribution. We fit to the sum of phase space $\pi^+\pi^0\omega$ MC and $\rho^+\omega$ MC. The fit result suggests that 0.52 ± 0.30 of the $D_s^+ \rightarrow \pi^+\pi^0\omega$ decay come from the $D_s^+ \rightarrow \rho^+\omega, \rho^+ \rightarrow \pi^+\pi^0$ decay. The points are the data and the superimposed line is the fit.

TABLE II: Branching fractions and upper limits. Uncertainties are statistical and systematic, respectively.

Mode	$\mathcal{B}_{\text{mode}}(\%)$
$D_s^+ \rightarrow \pi^+\omega$	$0.21 \pm 0.09 \pm 0.01$
$D_s^+ \rightarrow \pi^+\pi^0\omega$	$2.78 \pm 0.65 \pm 0.25$
$D_s^+ \rightarrow \pi^+\pi^+\pi^-\omega$	$1.58 \pm 0.45 \pm 0.09$
$D_s^+ \rightarrow \pi^+\eta\omega$	$0.85 \pm 0.54 \pm 0.06$
	< 2.13 (90% CL)
$D_s^+ \rightarrow K^+\omega$	< 0.24 (90% CL)
$D_s^+ \rightarrow K^+\pi^0\omega$	< 0.82 (90% CL)
$D_s^+ \rightarrow K^+\pi^+\pi^-\omega$	< 0.54 (90% CL)
$D_s^+ \rightarrow K^+\eta\omega$	< 0.79 (90% CL)

most of the D_s inclusive ω decays $(6.1\pm 1.4)\%$ [1]. We also report the first upper limits on $D_s^+ \rightarrow K^+\omega$, $D_s^+ \rightarrow K^+\pi^0\omega$, $D_s^+ \rightarrow K^+\pi^+\pi^-\omega$, and $D_s^+ \rightarrow K^+\eta\omega$ decays.

We gratefully acknowledge the effort of the CESR staff in providing us with excellent luminosity and running conditions. This work was supported by the A.P. Sloan Foundation, the National Science Foundation, the U.S. Department of Energy, the Natural Sciences and Engineering Research Council of Canada, and the U.K. Science and Technology Facilities Council.

-
- [1] S. Dobbs *et al.* (CLEO Collaboration), arXiv:0904.2417, accepted by Phys. Rev. D.
 - [2] C. Amsler *et al.* (Particle Data Group), Phys. Lett. B **667**, 1 (2008).
 - [3] M. Gronau and J. L. Rosner, Phys. Rev. D **79**, 074006 (2009); **79**, 074022 (2009).
 - [4] D. Cronin-Hennessy *et al.* (CLEO Collaboration), arXiv:0801.3418.
 - [5] R. A. Briere *et al.* (CESR-c and CLEO-c Taskforces, CLEO-c Collaboration), Cornell University, LEPP Report No. CLNS 01/1742 (2001) (unpublished).
 - [6] Y. Kubota *et al.* (CLEO Collaboration), Nucl. Instrum. Meth. A **320**, 66 (1992).
 - [7] D. Peterson *et al.*, Nucl. Instrum. Methods Phys. Res., Sec. A **478**, 142 (2002).
 - [8] M. Artuso *et al.*, Nucl. Instrum. Methods Phys. Res., Sec. A **502**, 91 (2003).
 - [9] S. Dobbs *et al.* (CLEO Collaboration), Phys. Rev. D **76**, 112001 (2007).
 - [10] R. Brun *et al.*, GEANT 3.21, CERN Program Library Long Writeup W5013 (unpublished) 1993.
 - [11] D.J. Lange, Nucl. Instrum. Methods Phys. Res., Sec. A **462**, 152 (2001).
 - [12] E. Barberio and Z. Was, Comput. Phys. Commun. **79**, 291 (1994).
 - [13] G. S. Adams *et al.* (CLEO Collaboration), Phys. Rev. Lett. **99**, 191805 (2007).
 - [14] P. U. E. Onyisi *et al.* (CLEO Collaboration), Phys. Rev. D **79**, 052002 (2009).